Abstract

Because poly-L-lysine (PLL) can exist in the α-helix or β-sheet conformation depending on solution preparation and solution conditions, PLL is a suitable candidate to probe the dependence of protein interactions on secondary structure. The osmotic second virial coefficient and weight-average molecular weight are reported from low-angle laser-light scattering measurements for PLL as a function of NaCl concentration, pH, and α-helix or β-sheet content. Interactions between PLL molecules become more attractive as salt concentration increases due to screening of PLL charge by salt ions and at low salt concentration become more attractive as pH increases due to decreased net charge on PLL. The experimental results show that interactions are stronger for the β-sheet conformation than for the α-helix conformation. A spherically-symmetric model for the potential of mean force is used to account for specific interactions not described by DLVO theory and to show how differences in secondary structure affect PLL interactions.

keywords: poly-L-lysine, potential of mean force, alpha helix, beta sheet, specific interactions

1. Introduction

Aggregation and precipitation of proteins from aqueous solution have important implications for industry and medicine. Salt-induced protein precipitation is a common first-step method for the recovery and purification of proteins from solution. Currently, empirical correlations and trial-and-error methods are used to adjust solution conditions for the precipitation of proteins. A molecular-thermodynamic model for the prediction of protein phase behavior would benefit design of more efficient purification processes. Development of such a model requires a quantitative understanding of how protein interactions depend on protein properties and solution conditions.

Aggregation of proteins is critical in several human disease states including cataract formation, Huntington's disease, Mad Cow disease, and Alzheimer's disease [1-3]. For example, the pathogenesis of Alzheimer's disease is believed to arise from the conformational alteration and fibril formation of β-amyloid protein, a 4-kDa peptide derived from proteolytic cleavage of the membrane-bound amyloid precursor protein (APP) [4,5]. It appears that the APP form β-sheet structures that aggregate into protofibrils [6-8]. The protofibrils lengthen and associate to form fibrils, eventually precipitating in the brain parenchyma causing cell death. Knowledge concerning how intermolecular forces depend on protein secondary-structure may provide insight into the pathogenesis of these diseases.

This work concerns efforts to understand how the secondary structure of the homopolymer poly-L-lysine (PLL) affects polymer-polymer interactions. The conformational states of PLL in aqueous solutions have been studied extensively and are shown to depend on a wide range of solution conditions including temperature, pH, salt concentration, and organic solvent content [9-14]. At neutral pH, PLL exists as a random coil in solution due to the high charge of the lysine side chains. Above pH 10.6, PLL transforms into the α-helix conformation because the charge on PLL is reduced at a pH above the pKa (10.5) of the lysine side chains. Upon heating PLL to 51^{o}C followed by slow cooling to room temperature at a pH above 10.6, the α-helix structure transforms into the β-sheet conformation [16]. Because the primary chemical

structure remains identical during this thermal process, PLL provides an ideal system to probe the effects of protein secondary-structure on protein-protein interactions.

In this study, we examine interactions between PLL in the α-helix conformation or β-sheet conformation using low-angle laser-light scattering (LALLS). The osmotic second virial coefficient and weight average molecular weight of PLL were determined in aqueous solutions as a function of NaCl concentration and pH for the α-helix and β-sheet conformations of PLL. As a first approximation, we propose a spherically-symmetric potential-of-mean-force model that contains DLVO terms and an attractive square-well potential. The difference in conformation (α-helix or β-sheet) affects the depth of the square well.

2. Materials and Methods

2.1 Poly-L-Lysine Solution Preparation

Poly-L-lysine hydrochloride (Lot. 38H5902), NaCl, and NaOH were purchased from Sigma (St. Louis, MO). Syringe-tip 0.1-μm pore-size filters and 3000 dalton cut-off ultrafiltration membranes were purchased from Millipore (Bedford, MA). Deionized water was obtained from a Barnstead-Nanopure II filtration unit.

An aqueous NaCl stock solution was prepared with deionized water. PLL was dissolved in 10 ml of the stock solution and the pH was adjusted with an aqueous 2M NaOH solution to the desired value. The volume of NaOH solution added was noted and the salt concentration and pH of the NaCl stock solution were adjusted accordingly. PLL samples of varying polymer concentration were prepared through dilution of the PLL stock solution with the NaCl stock solution. The final pH of the PLL solutions, checked before and after LALLS measurements, agreed within 0.1 pH units. The concentration of PLL was determined after the LALLS data collection by measuring absorbance at 221.3 nm and 25^{o}C using a Beckman DU-6 spectrophotometer with an extinction coefficient of 2.711 L/g-cm.

The secondary structure of PLL solutions was determined by cicular-dichroism spectropolarimetry (CD). Because the concentration of PLL solutions was too high for CD measurements, they were diluted by an aqueous NaCl solution of the same pH. The concentration of NaCl was kept below 0.04 M to minimize the signal-to-noise ratio measured by CD. Simple dissolution of PLL in aqueous NaCl solutions at pH above 11.2 showed that PLL was completely α-helical in structure.

The aqueous PLL salt-solution was heated to 51^{o}C and cooled to room temperature over the course of 4 hours to obtain the β-sheet conformation. Aggregation of PLL was visible at this high temperature. As the solution is heated, the α-helix form of PLL unfolds into the random coil conformation. Due to the relatively high concentration of the PLL solution (~5 g/L), aggregation of the unfolded PLL occurred with formation of a gelatinous precipitate. Therefore, the PLL solution was diluted 25 fold with the stock salt solution and 10% methanol to minimize the extent of aggregation of the unfolded form of PLL. The concentration of methanol was kept low because methanol induces PLL into the α-helix conformation at high concentrations [10].

The diluted PLL solution was heated and cooled as described above and concentrated using an Amicon Ultrafiltration Unit with 3000 dalton cut-off membranes. To minimize the concentration of methanol in the PLL solution, the concentrated PLL solution was further diluted with the aqueous NaCl stock solution and concentrated again. This process was repeated twice with an estimated final methanol concentration of less than 1%. The pH of the PLL solution was adjusted after the ultrafiltration process. Samples of varying PLL concentration were prepared as described above. The β-sheet form of PLL was confirmed by CD after LALLS measurements.

2.2 Low-Angle Laser Light (LALLS) Measurements

LALLS allows for the determination of the weight-average molecular weight and the osmotic second virial coefficient (B_{22}) in dilute solution. For a system containing water (1), polymer (2), and salt (3), the light-scattering equation is given by [17]:

$$\frac{Kc_2(\partial n/\partial c_2)^2_{T,\mu}}{\overline{R}_\theta} = \frac{1}{M_2} + 2B_{22}c_2 \qquad (1)$$

where $\overline{R_\theta}$ is the excess Rayleigh scattering of the polymer solution over the salt solution and K is the light-scattering constant given by $2\pi^2 n^2/N_A\lambda^4$, where λ is the wavelength of laser light, n is the refractive index of the solvent, M_2 is the polymer molecular weight, N_A is Avagadro's number, and c_2 is the polymer mass concentration. B_{22} and M_2 can be determined by plotting $Kc_2(\partial n/\partial c_2)^2_{T,\mu}/R_\theta$ versus c_2.

Because PLL is polydisperse, every molecular size must be considered separately in the derivation of the excess scattering Rayleigh ratio, R_θ. The refractive index increment, $(\partial n/\partial c)_{T,\mu(d)}$, at constant temperature and constant solvent chemical potential, μ, is similar for all proteins and can be approximated by an average value leading to the following light scattering equation [18]:

$$\frac{Kc_s(\partial n/\partial c_s)^2_{T,\mu}}{\overline{R}_\theta} = \frac{1}{M_w} + 2B_{avg}c_s \qquad (2)$$

where c_s is the total polymer mass concentration, M_w is the weight-average molecular weight, and B_{avg} is an averaged osmotic second virial coefficient that is a weighted function of all B_{ij}s:

$$B_{avg} = \frac{1}{\langle M_w \rangle^2} \sum_i \sum_j M_i M_j w_i w_j B_{ij} \qquad (3)$$

where w_i is the weight fraction of species i.

LALLS data were obtained using a Minidawn light scattering instrument from Wyatt Technology (Santa Barbara, CA). A 30-mW semiconductor diode laser (λ = 690 nm) is focused into a flow cell, and passes in

the same direction as that of the flowing stream. The instrument contains three detectors that collect scattered light at scattering angles 41.5°, 90°, and 138.5° in water. The system was run in batch mode where a PLL sample was continuously injected at a flow rate of 0.1 ml/min by a syringe pump. Data were collected for a given salt concentration and pH while varying the PLL concentration. A Zimm-plot analysis gives B_{avg} and M_w according to Eq. (2).

The PLL solution was collected from the flow cell after measurements. The measured pH was within 0.1 pH units compared to the initial pH. The concentration of PLL was determined by uv spectrophotometry as noted above.

3. Results

Low-angle laser-light scattering data were collected for solutions of poly-L-lysine in the α-helix conformation for the pH range 11.2 to 11.8 and NaCl concentrations 0.3 to 1.03 M. Data were collected for PLL in the β-sheet conformation for the same pH range at 0.03 M NaCl but not at higher salt concentration where we observed aggregation. Secondary structural information for PLL was obtained from circular-dichroism measurements as described above; representative results are given in Fig.1. Simple dissolution of PLL in aqueous NaCl solutions led to formation of the α-helix structure, while heating and slow cooling of these solutions lead to the β-sheet conformation.

Table 1 shows osmotic second virial coefficients as a function of solution conditions obtained from a Zimm-plot analysis of LALLS data. The measured weight-average molecular weight is 20300 ± 500 daltons for the α-helix conformation and 18700 ± 600 daltons for the β-sheet conformation. The lower M_w for the β-sheet conformation is probably due to base hydrolysis of PLL amide bonds during the heating

$$pH = pKa + \log\frac{[LYS]}{[LYS^+]} \qquad (4)$$

process. Although the pH of all solutions is above the pKa of the lysine side chain (10.5), there is still significant positive charge on PLL. The charge was calculated from the Henderson-Hasselbalch equation:

where, $[LYS]$ and $[LYS^+]$ represent the concentration of lysine residues in the proton-acceptor and proton-donor states respectively. The number of lysine residues was calculated from the ratio of M_w to the weight of a single lysine residue (128.17 daltons). Table 2 gives the calculated charge of PLL as a function of pH. The charge of PLL is important for explaining the observed trends of B_{avg}.

In Fig. 2, B_{avg} is plotted as a function of NaCl concentration for PLL in the α-helix conformation. At fixed pH, B_{avg} declines (indicating greater PLL-PLL interactions) as the salt concentration increases due to rising charge screening between PLL molecules by salt ions. In Fig. 3, B_{avg} is plotted as a function of pH for PLL in the α-helix and β-sheet conformations. At fixed salt concentration, B_{avg} decreases with rising pH due to lower net charge (lower repulsive-charge interactions) of PLL at higher pH. Interactions for the β-sheet conformation are attractive for all pH values and greater than those for the α-helix conformation.

Differences in PLL interactions for the α-helix and β-sheet conformations arise from differences in secondary structure since the primary chemical structure is identical for both conformations. As a simplification, the α-helix and β-sheet conformations can be thought of as a cylinder and a flat surface, respectively. Specific attractive-interactions are predominantly hydrophobic interactions of uncharged lysine side chains. The extent of possible surface-to-surface contact is greater for two flat surfaces compared to that for two cylinders. Therefore, hydrophobic interactions for the flat surface are greater than those for the cylinder, providing larger attractive interactions for the β-sheet conformation as indicated by B_{avg}.

4. Discussion

4.1 A Model for the Potential of Mean Force for Poly-L-lysine

A potential of mean force (PMF) model is proposed to represent experimental measurements of the osmotic second virial coefficient for PLL as a function of solution conditions. The osmotic second virial coefficient can be related to the PMF by:

$$B_{ave} = -\frac{1}{2}\frac{N_A}{M_w^2}\int_0^\infty 4\pi r^2 (\exp[-W(r)/kT] - 1)\, dr \qquad (5)$$

where the PMF, W(r), is an average because the PLL solutions are polydisperse [19].

The PMF describes the force between two solute molecules at infinite dilution, averaged over all configurations of the solvent molecules [20]. The primary contributions are repulsive charge-charge interactions, attractive dispersion forces, and specific interactions arising from the hydrophobic nature of the uncharged lysine residues. The PMF also depends on the size and shape of the PLL molecules. As a first approximation, PLL molecules are modeled as interacting hard spheres of uniform size. The PMF is given by a sum of pairwise potentials:

where r is the center-to-center distance between PLL molecules, $W_{hs}(r)$ is the hard-sphere potential, $W_{elec}(r)$

$$W(r) = W_{hs}(r) + W_{elec}(r) + W_{disp}(r) + W_{spec}(r) \qquad (6)$$

is the electric double-layer-repulsion potential, $W_{disp}(r)$ is the dispersion potential, and $W_{spec}(r)$ is a square-well potential that accounts for hydrophobic interactions.

The hard-sphere potential is given by:

$$W_{hs}(r) = \begin{bmatrix} \infty & for & r \le \sigma \\ 0 & for & r > \sigma \end{bmatrix} \qquad (7)$$

where σ is the effective hard-sphere diameter of PLL [21]. The hard sphere diameter can be calculated from the following:

$$\sigma = 2\left(\frac{3\upsilon M_{avg}}{4\pi N_A}\right)^{\frac{1}{3}} \tag{8}$$

where υ is the partial specific volume chosen to be 0.75 ml/g, typical of values for proteins [22].

The electric double-layer repulsion is derived from Debye-Hűckel theory [21]:

$$W_{elec}(r) = \frac{z^2 e^2 \exp[-\kappa(r-\sigma)]}{4\pi\varepsilon_o\varepsilon_r(1+\kappa\sigma/2)^2} \qquad for \;\; r > \sigma \tag{9}$$

where z is the valence of PLL, e is the elementary charge, $4\pi\varepsilon_o$ is the dielectric permittivity of free space, and ε_r is the relative dielectric permittivity of water; κ is the inverse Debye length given by:

$$\kappa^2 = \frac{2e^2 N_A I}{kT\varepsilon_o\varepsilon_r} \tag{10}$$

where I is the ionic strength of the solution, k is Boltzmann's constant, and T is temperature.

The attractive dispersion potential can be approximated by:

$$W_{disp}(r) = -\frac{H}{36}\left(\frac{\sigma}{r}\right)^6 \tag{11}$$

where H is the effective Hamaker constant for peptide-peptide interactions. The Hamaker constant is primarily a function of the chemical composition of the polymer; it is on the order of $5kT$ for protein molecules [23]. The dispersion force is not a function of solution salt concentration because the time scale for electron fluctuations between atoms causing dispersion forces is much shorter than that for ion rearrangement in the double layer [24].

The square-well potential is given by:

$$W_{spec}(r) = \begin{bmatrix} -\varepsilon_{spec} & for & \sigma \le r \le \sigma + \delta \\ 0 & for & \sigma + \delta < r \end{bmatrix} \quad (12)$$

where ε_{spec} is the depth of the square well and δ is the width of the square well. The primary specific interaction is the hydrophobic interaction due to the hydrophobic nature of the lysine side chains. Because the osmotic second virial coefficient accounts for interactions between two PLL molecules, a value of 0.134σ was chosen for δ to ensure that association is only for the reaction 2(monomer) □ dimer [25].

Eqs. (5) through (12), in conjunction with the experimentally-measured osmotic second virial coefficients, were used to calculate ε_{spec} as a function of pH, salt concentration, and PLL conformation. The net charges on PLL in Table 2 were used to calculate $W_{elec}(r)$ as described earlier. The equivalent hard sphere diameter of PLL (σ) was calculated from equation 8 using the experimentally-determined M_w. The average values of σ for the α-helix and β-sheet conformations are 35.6 and 34.7 Å, respectively.

4.2 PMF Model Results

The specific interaction energy term, ε_{spec}/kT, takes into account hydrophobic interactions between PLL molecules and any charge-charge and dispersion interactions not included in the electric double-layer and dispersion potentials. Table 3 gives ε_{spec}/kT values. These are plotted as a function of solution pH in Fig. 4.

For the α-helix conformation of PLL, ε_{spec}/kT is not a function of salt concentration above 0.103 M NaCl; the average is $2.2kT$. At intermediate and high salt concentrations, the electric double-layer does not contribute significantly to the total potential due to charge screening by salt ions. Because the dispersion potential is not a function of pH or salt concentration, this contribution remains constant for all solution conditions; it is only a function of the size of the PLL molecules. The specific square-well contribution is

much larger than the dispersion contribution. Therefore, ε_{spec}/kT can be attributed to hydrophobic interactions on the order of 2.2 *kT*.

At a salt concentration of 0.03 M NaCl, ε_{spec}/kT for the α-helix and β-sheet conformations appears to be a strong function of pH. The change in polymer charge from pH 11.2 to 11.8 is approximately +18. At low salt concentrations, because the electric double-layer potential is dominant relative to the dispersion potential, ε_{spec}/kT may be a function of solution pH because PLL is more hydrophobic at pH 11.8 than at 11.2. Therefore, ε_{spec}/kT may increase with pH. This trend however is not observed in the data presented in Figure 4.4. The values for ε_{spec}/kT do not depend on solution pH at higher salt concentrations.

Error may result from applying a spherically-symmetric electric double-layer potential. The spherical model overpredicts the extent of charge-charge repulsion between PLL molecules; therefore, large ε_{spec}/kT values are required to overcome this repulsion. Further, PLL was represented as a hard sphere with a specific volume of a typical protein molecule. The extended conformations of the α-helix and β-sheet forms of PLL may be different from those of a typical protein. A larger hard-sphere diameter produces less charge-charge repulsion.

The specific energies ε_{spec}/kT for the β-sheet conformation always lie above those for the α-helix conformation at similar salt concentrations. The hydrophobic interaction appears to be much greater for the β-sheet conformation. Because the electric double-layer potential overpredicts charge-charge repulsion, comparison of ε_{spec}/kT should be made at pH 11.8 where the effect of charge is minimal. The difference between ε_{spec}/kT values at 0.03M and 1.0M (pH 11.8) for the α-helix conformation is 0.6*kT*. The value of ε_{spec}/kT is roughly 2.5 times greater for the β-sheet conformation compared to that for the α-helix conformation (pH 11.8). Larger hydrophobic interactions result from the larger surface-to-surface contact area for the β-sheet conformation compared to that for the α-helix conformation.

5. Conclusions

Interactions between PLL molecules depend on secondary structure. The β-sheet conformation exhibits greater attractive interactions compared to the α-helix conformation for similar solution conditions. Using a spherically symmetric PMF model, the magnitude of the specific hydrophobic interactions is roughly 2.5 times greater for the β-sheet conformation. Development of a PMF model for cylinders or surfaces representing the α-helix or β-sheet, respectively, may provide further insight into the nature of these specific interactions. Because transformation of proteins to the β-sheet structure with subsequent aggregation is believed to be the cause of several disease states, better understanding of this aggregation may lead to design of small-molecule drugs to prevent such aggregation.

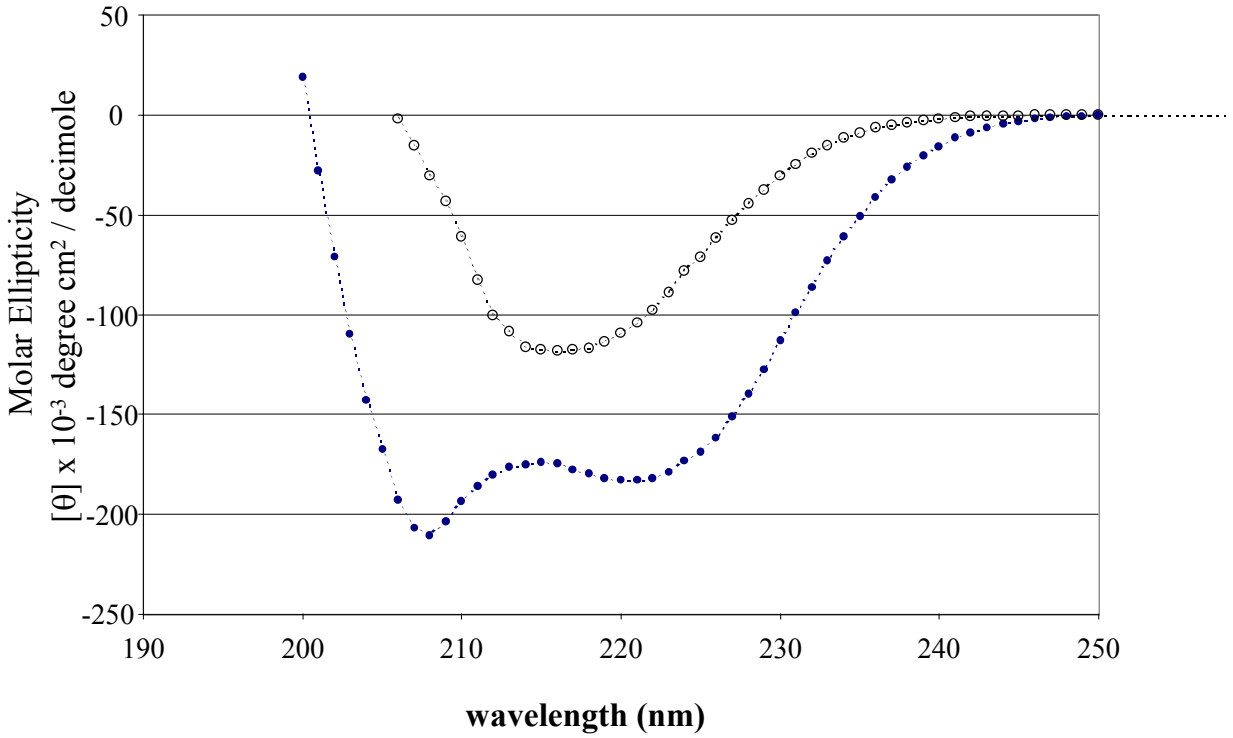

Fig. 1. Far-UV circular dichroism spectra of poly-L-lysine at pH 11.5 in 0.03 M aqueous NaCl solution in the α-helix (•) and β-sheet (○) conformations.

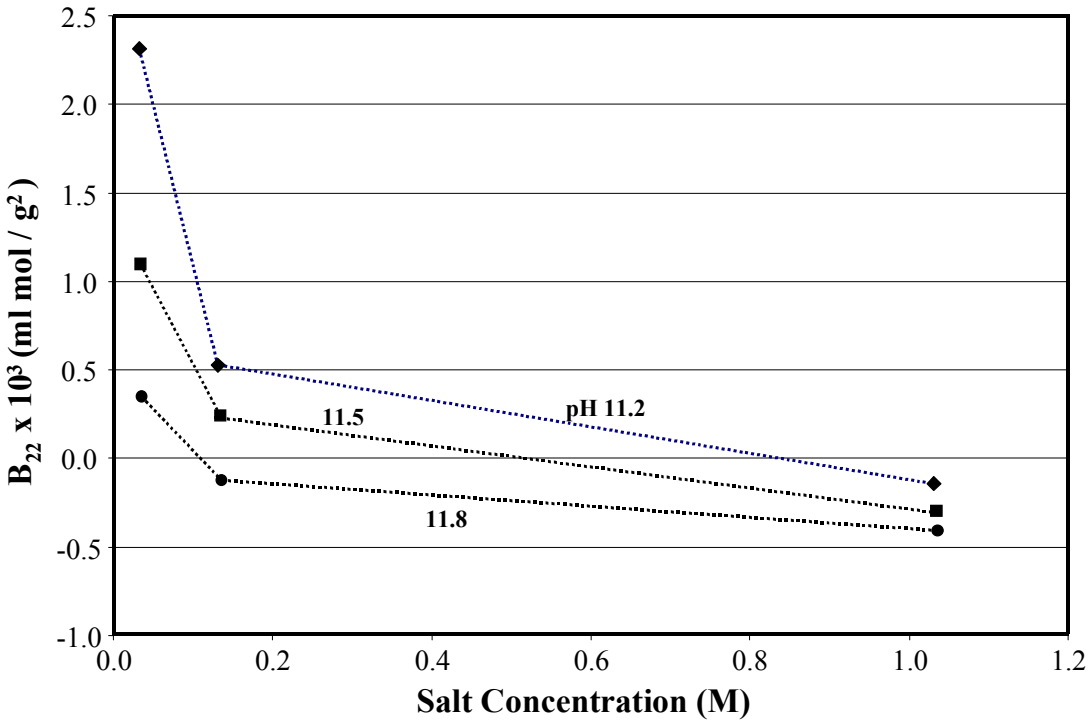

Fig. 2. Osmotic second virial coeffients (B_{22}) plotted as a function of NaCl concentration determined by low-angle laser-light scattering for poly-L-lysine in the α-helix conformation.

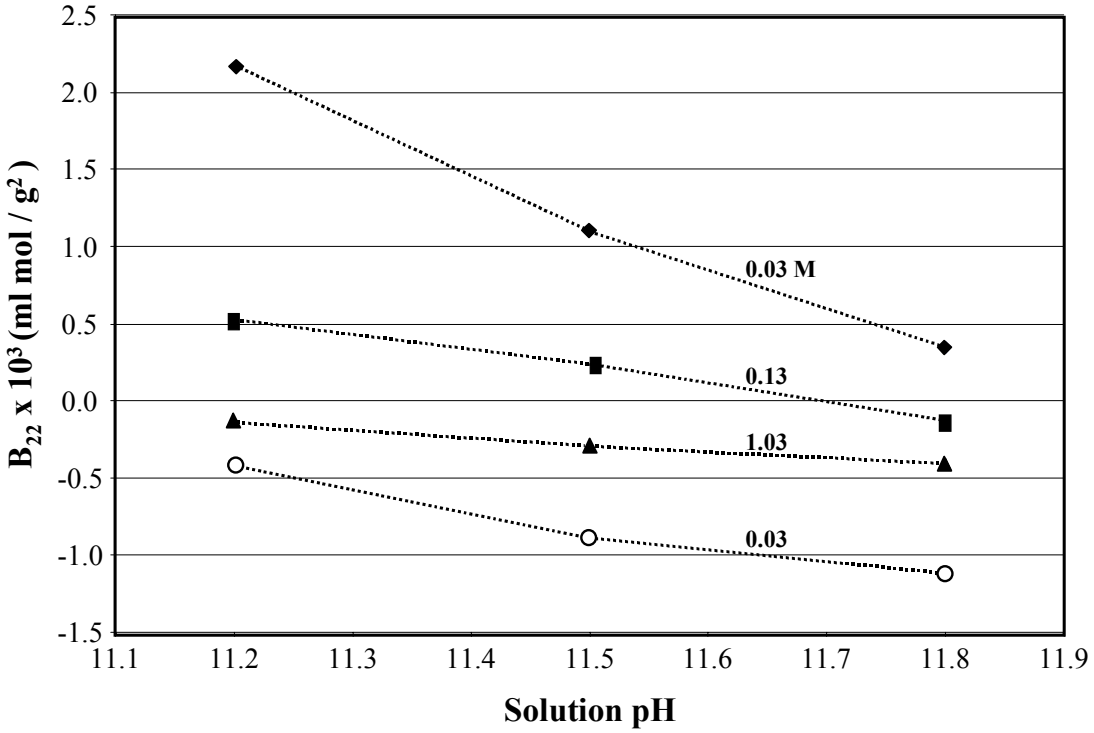

Fig. 3. Osmotic second virial coeffients (B_{ave}) as a function of solution pH determined by low-angle laser-light scattering for poly-L-lysine in aqueous NaCl solutions. Filled symbols represent PLL in the α-helix conformation and open symbols (○) represent PLL in the β-sheet conformation.

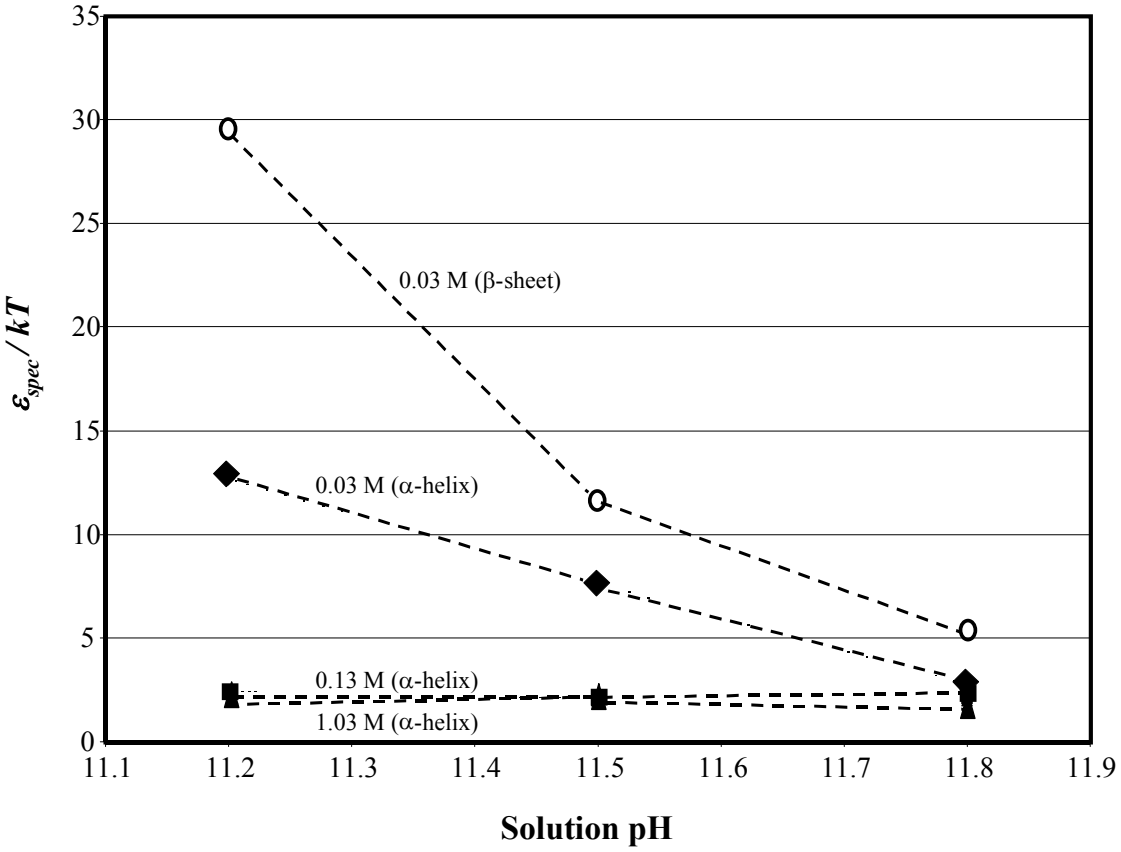

Fig. 4. Calculated values of ε_{spec}/kT for poly-L-lysine as a function of solution pH in aqueous NaCl solutions. Open symbols represent the β-sheet conformation and filled symbols represent the α-helix conformation.

α-helix conformation

pH	NaCl concentration (M)	B_{22} x 10^3 (ml mol/ g^2)
11.2	0.032	2.32
	0.132	0.52
	1.032	-0.14
11.5	0.034	1.10
	0.134	0.24
	1.034	-0.29
11.8	0.036	0.35
	0.136	-0.13
	1.036	-0.41

β-sheet conformation

pH	NaCl concentration (M)	B_{22} x 10^3 (ml mol/ g^2)
11.2	0.032	-0.42
11.5	0.134	-0.89
11.8	1.036	-1.117

Table 1. Osmotic second virial coefficient (B_{ave}) of poly-L-lysine in aqueous NaCl solutions from low-angle laser-light scattering measurements.

α-helix conformation

pH	Net Charge
11.2	26.4
11.5	14.4
11.8	7.6

β-sheet conformation

pH	Net Charge
11.2	24.3
11.5	13.3
11.8	7.0

Table 2. Net charge on PLL calculated from M_w and the mass of a lysine residue using the Henderson-Hasselbalch equation.

α-helix conformation

pH	NaCl concentration (M)	ε_{spec}/kT
11.2	0.032	12.7
	0.132	2.4
	1.032	2.3
11.5	0.034	7.6
	0.134	2.2
	1.034	2.0
11.8	0.036	2.8
	0.136	2.1
	1.036	2.0

β-sheet conformation

pH	NaCl concentration (M)	ε_{spec}/kT
11.2	0.032	29.5
11.5	0.134	11.7
11.8	1.036	5.4

Table 3. Values for ε_{spec}/kT for poly-L-lysine in aqueous NaCl solutions from a square well potential-of-mean-force model.

Acknowledgments

This work was supported by the National Science Foundation CT59530793 and by the Director, Office of Science, Office of Basic Energy Sciences, Chemical Sciences Division of the U.S. Department of Energy under Contract Number DE-AC0376SF0009.

References

[1] G. Forloni, N. Angeretti, R. Chiesa, E. Monzani, M. Salmona, O. Bugiani and F. Tagliavini, Neurotoxicity of a prion protein-fragment, Nature 362 (1993) 543-546.

[2] E. E. Wanker, Protein aggregation and pathogenesis of Huntington's disease: Mechanisms and correlations, Biol. Chem. 381 (2000) 937-942.

[3] L. Takemoto and D. Boyle, The possible role of alpha-crystallins in human senile cataractogenesis, Int. J. Biol. Macromol. 22 (1998) 331-337.

[4] C. L. Masters, G. Simms, N. A. Weinman, G. Multhaup, B. L. McDonald and K. Beyreuther, Amloid plaque core protein in Alzheimer disease and down syndrome, Proc. Natl. Acad. Sci. USA 82 (1985) 4245-4249.

[5] J. Kang, H. G. Lemaire, A. Unterbeck, J. M. Salbaum, C. L. Masters, K. H. Grzeschik, G. Multhaup, K. Beyreuther and B. Muller-Hill, The precursor of Alzheimer's disease amyloid A4 protein resembles a cell-surface receptor, Nature 325 (1987) 733-735.

[6] D. M. Walsh, A. Lomakin, G. B. Benedek, M. M. Condron and D. B. Teplow, Amyloid β-protein fibrillogenesis: detection of a protofibrillar intermediate, J. Biol. Chem. 272 (1997) 22364-22372.

[7] J. D. Harper, C. M. Lieber and P. T. Lansbury, Atomic force microscopic imaging of seeded fibril formation and fibril branching by the Alzheimer's disease amyloid β-protein, Chem. Biol. 4 (1997) 951-959.

[8] C. L. Shen and R. M. Murphy, Solvent effects on self-assembly of β-amyloid peptide, Biophys. J. 69 (1995) 640-651.

[9] J. Hermans, Effect of protein denaturants on stability of alpha helix, J. Amer. Chem. Soc. 88 (1966) 2418.

[10] R. F. Epand and H. A. Scheraga, Helix-coil transition of poly-l-lysine in methanol-water solvent mixtures, Biopol. 6 (1968) 1383.

[11] T. J. Yu, J. L. Lippert and W. L. Peticola, Laser Raman studies of conformational variations of poly-l-lysine, Biopol. 12 (1973) 2161-2176.

[12] A. K. Mishra and J. C. Ahluwalia, Alcohol induced conformational transitions of proteins and polypeptides - thermodynamic studies of some model compounds, Int. J. Pep. Pro. Res. 21 (1983) 322-330.

[13] M. Satoh, T. Hirose and J. Komiyama, Solvent-induced and salt-induced coil helix transition of poly(l-lysine) salts in water-alcohol mixtures, Pol. 34 (1993) 4762-4766.

[14] A. I. Arunkumar, T. K. S. Kumar, T. Sivaraman and C. Yu, Acetonitrile-induced conformational transitions in poly-l-lysine, Int. J. Biol. Macromol. 21 (1997) 299-305.

[15] A. I. Arunkumar, T. K. S. Kumar and C. Yu, Specificity of helix-induction by 2,2,2-trifluoroethanol in polypeptides, Int. J. Biol. Macromol. 21 (1997) 223-230.

[16] N. Greenfield and G. D. Fasman, Computed circular dichroism spectra for evaluation of protein conformation, Biochem. 8 (1969) 4108.

[17] W. H. Stockmayer, Light scattering in multi-component systems, J. Chem. Phys. 18 (1950) 58-61.

[18] H. Yamakawa, Modern theory of polymer solutions. (Harper and Row Publishers, New York, 1971).

[19] T. L. Hill, Theory of solutions, J. Amer. Chem. Soc. 79 (1957) 4885-4890.

[20] W. G. McMillan and J. E. Mayer, The statistical thermodynamics of multicomponent systems, J. Chem. Phys. 13 (1945) 276-305.

[21] E. J. W. Verwey and J. T. K. Overbeek, Theory of lyophobic colloids (Elsevier, Amsterdam, 1948).

[22] T. E. Creighton, Proteins: stuctures and molecular properties (W. H. Freeman and Company, New York, 1993).

[23] S. Nir. Van der Waals interactions between surfaces of biological interest, Prog. Surf. Sci. 8 (1976) 1-58.

[24] J. Israelachvili, Intermolecular and surface forces (Academic Press, San Diego, 1991).

[25] M. S. Wertheim, Fluids of dimerizing hard spheres and fluid mixtures of hard spheres and dispheres, J. Chem. Phys. 85 (1986) 2929-2936.

Effect of Secondary Structure on the Potential of Mean Force for Poly-L-Lysine in the α-Helix and β-sheet Conformations

J. J. Grigsby[(1)], H. W. Blanch[(1)], J. M. Prausnitz[(1,2)]

(1) Chemical Engineering Department
University of California,
Berkeley, CA 94720

(2) Chemical Sciences Division,
Lawrence Berkeley National Laboratory,
Berkeley, CA 94720

Number of pages 27

Number of tables 3

Number of figures 4